

## Supplementary Methods

### Examination of lineage plasticity of hepatocytes and cholangiocytes in HBTOs

Tomato<sup>+</sup> SHs and wild type cholangiocytes, or wild type SHs and Tomato<sup>+</sup> cholangiocytes were used for inducing HBTOs. After a month of co-culture, images were taken of three different wells for each combination of cultures on a confocal microscope. Tomato<sup>+</sup> cells were counted in the images. For the co-culture of Tomato<sup>+</sup> SHs and wild type cholangiocytes, CK19 was used to find Tomato<sup>+</sup>CK19<sup>+</sup> cells, which suggest hepatocyte-to-cholangiocyte conversion proceeds in HBTOs. For co-culture of wild type SH and Tomato<sup>+</sup> cholangiocytes, HNF4 $\alpha$  was used to find Tomato<sup>+</sup>HNF4 $\alpha$ <sup>+</sup> cells, which suggest cholangiocyte-to-hepatocyte conversion proceeds in HBTOs.

### Culture of MHs

MHs were isolated from mouse liver using two-step collagenase perfusion. The MHs were plated in 24-well plates coated with type I collagen at a density of  $1 \times 10^5$  cells/well. CYP3A4-like activity was measured one and five days after plating.

### Gene expression analysis

To analyze the expression of cholangiocyte markers in HBTOs, collagen gel containing HBTOs was isolated from one well of a 24-well plate, 500  $\mu$ l of lysis solution was added, and the solution was homogenized with a homogenizer. Total RNA was prepared using RNeasy mini kits, according to the manufacturer's protocol (Qiagen, Hilden, Germany). RNA was quantified using a NanoDrop spectrophotometer (Thermo Fisher Scientific, Waltham, MA), and 50 ng of total RNA was used to synthesize cDNA using PrimeScript 1<sup>st</sup> strand cDNA synthesis kits (Takara Bio Inc., Shiga, Japan). Quantitative PCR was performed using an ABI PRISM 7500 (Thermo Fisher, Scientific) with the primers shown in **Table S4**.

### **Isolation of cells from HBTOs**

HBTOs were generated in 12-well plates. Four weeks after Co-MG overlay, gels containing HBTOs were transferred from 3 wells into 15 ml tube. Two ml of Cell Recovery Solution (BD biosciences) was added, and the solution was incubated for 30 min on ice. Gels were broken down by pipetting and 8 ml of culture medium was added. After centrifugation for 4 min at  $150 \times g$ , the pellet was resuspended in 2 ml PBS containing Liberase TM (Roche) and incubated at 37°C for 15 min. Gels were dissolved by further pipetting and centrifuged for 4 min at  $150 \times g$ . Cells were incubated with FITC-conjugated anti-EpCAM antibody. EpCAM(–) and (+) cells were isolated on a MoFlow (Beckman coulter, Brea, CA).

### **Uptake of Rho123 to the biliary tissue in HBTOs**

HBTOs cultured for four weeks after Col-MG overlay were further incubated with medium containing 10  $\mu$ M Rho123 (FUJIFILM Wako Pure Chemical Corporation) for 30 min with or without verapamil (Sigma-Aldrich). Wells were washed with medium five times, and images were taken on a fluorescence microscope.

### **Effect of forskolin on biliary tissue in HBTOs**

HBTOs cultured for four weeks after Col-MG overlay were further incubated in the presence of forskolin (FUJIFILM Wako Pure Chemical Corporation). Images were taken 0 and 1 hour after forskolin treatment. To estimate the extent of lumen expansion, the brightly colored luminal areas were extracted and quantified using ImageJ.

### **RNA sequence analysis**

SHs and MHs were isolated from three healthy adult mice. SHs were further purified as CD31<sup>-</sup> CD45<sup>-</sup>EpCAM<sup>-</sup>ICAM-1<sup>+</sup> cells using a FACS AriaII flow cytometer. Total RNA was extracted using RNeasy Mini kits (Qiagen). Poly(A) RNAs were purified and cDNA libraries were constructed using Ion Total RNA-Seq Kits v2 (ThermoFisher). RNA sequencing was performed using an Ion Proton system (ThermoFisher).

### **Immunostaining of liver tissue**

Fetal and adult liver tissues were fixed in PBS containing 4% paraformaldehyde at 4°C. After embedding in OCT compound, 7 µm thick frozen sections were prepared using a cryostat (Leica, Wetzlar, Germany). Sections were permeabilized in PBS containing 0.2% Triton X-100 at room temperature for 5 min. After blocking in Block ACE, the samples were incubated with primary antibodies and then dye-conjugated secondary antibodies were applied. Nuclei were counterstained with Hoechst33342.

## Supplementary tables

**Table S1. Lineage of hepatocytes and cholangiocytes in HBTOs**

	Cell Count /Area (cells)		Ratio (%)	
Wt SH & Tomato <sup>+</sup> Cholangiocyte	Tomato <sup>+</sup> HNF4 $\alpha$ <sup>-</sup>	Tomato <sup>+</sup> HNF4 $\alpha$ <sup>low</sup>	Tomato <sup>+</sup> HNF4 $\alpha$ <sup>-</sup>	Tomato <sup>+</sup> HNF4 $\alpha$ <sup>low</sup>
	75 ± 16	1.0±0.5	98.6 ± 0.6	1.4 ± 0.6
Tomato <sup>+</sup> SH & Wt Cholangiocyte	Tomato <sup>+</sup> CK19 <sup>-</sup>	Tomato <sup>+</sup> CK19 <sup>+</sup>	Tomato <sup>+</sup> CK19 <sup>-</sup>	Tomato <sup>+</sup> CK19 <sup>+</sup>
	46±10	0	100	0

In co-cultures of wild type (Wt) SH and Tomato<sup>+</sup> cholangiocytes, some Tomato<sup>+</sup>HNF4 $\alpha$ <sup>+</sup> cells were detected, suggesting that cholangiocyte-to-hepatocyte conversion proceeds in HBTO. But HNF4 $\alpha$  expression in those cells was quite low and they maintained cellular morphology of cholangiocytes. In co-cultures of Tomato<sup>+</sup> SHs and Wt cholangiocytes, Tomato<sup>+</sup>CK19<sup>+</sup> cells were not observed, suggesting that hepatocyte-to-cholangiocyte conversion proceeds in HBTOs. Data are shown as Mean ± SEM.

**Table S2. Primary Antibodies**

Antibody	Company	Host animal	Method	Dilution
Albumin	Bethyl laboratory	goat	IF	1:1000
CD16/32	BD Pharmingen	rat	FACS	1:1000
CD31 (PE-Cy7-conjugated)	BD Pharmingen	rat	FACS	1:1000
CD45 (APC-Cy7-conjugated)	BD Pharmingen	rat	FACS	1:1000
CEACAM	R&D systems	sheep	IF	1:500
CLDN2	Proteintech	rabbit	IF	1:500
Cytokeratin 19	Tanimizu et al. 2003	rabbit	IF	1:2000
ECAD	BD biosciences	mouse	IF	1:1000
ECAD (PE-conjugated)	Biolegend	rat	FACS	1:1000
EpCAM	BD Pharmingen	rat	IF	1:500
EpCAM (FITC-conjugated)	Biolegend	rat	MACS	1:1000
EZRIN	Proteintech	rabbit	IF	1:500
HNF4 $\alpha$	Santa Cruz Biotechnology Inc.	rabbit	IF	1:200
HNF4 $\alpha$	Santa Cruz Biotechnology Inc.	goat	IF	1:200
ICAM-1 (PE-conjugated)	BD Pharmingen	rat	FACS	1:1000
OPN	R&D systems	goat	IF	1:500
RADIXN	Abcam	rabbit	IF	1:500
SOX9	Millipore	rabbit	IF	1:1000
ZO1	A gift from Dr. Bruce Stevenson (University of Alberta)	rat	IF	1:2000

**Table S3. Secondary Antibodies**

Antibody	Company	Host animal	Method	Dilution
AlexaFluor488 anti-rabbit IgG	ThermoFisher	Donkey	IF	1:1000
AlexaFluor555 anti-rabbit IgG	ThermoFisher Scientific	Donkey	IF	1:1000
AlexaFluor647 anti-rabbit IgG	ThermoFisher Scientific	Donkey	IF	1:1000
AlexaFluor488 anti-goat IgG	ThermoFisher Scientific	Donkey	IF	1:1000
AlexaFluor555 anti-goat IgG	ThermoFisher Scientific	Donkey	IF	1:1000
AlexaFluor633 anti-goat IgG	ThermoFisher Scientific	Donkey	IF	1:1000
AlexaFluor488 anti-sheep IgG	ThermoFisher Scientific	Donkey	IF	1:1000
Cy3 anti-sheep IgG	Jackson ImmunoResearch Laboratories Inc.	Donkey	IF	1:1000
AlexaFluor488 anti-rat IgG	ThermoFisher Scientific	Donkey	IF	1:1000
Cy5 anti-rat IgG	Jackson ImmunoResearch Laboratories Inc	Donkey	IF	1:1000
AlexaFluor488 Phalloidin	ThermoFisher Scientific	Donkey	IF	1:300
AlexaFluor555 Phalloidin	ThermoFisher Scientific	Donkey	IF	1:300
AlexaFluor633 Phalloidin	ThermoFisher Scientific	Donkey	IF	1:300

**Table S4. Primers used for PCR**

Gene name		Sequence
<i>Ae2</i>	Sense	5'-CAGCAAAGGGGCACAGAC-3'
	Antisense	5'-CACCTCCGTCGTCACCTC-3'
<i>Albumin</i>	Sense	5'-GAA AGC CCA CTG TCT TAG TG-3'
	Antisense	5'-GGG TGT AGC GAA CTA GAA TG-3'
<i>Axin2</i>	Sense	5'-GAGAGTGAGCGGCAGAGC-3'
	Antisense	5'-CGGCTGACTCGTTCTCCT-3'
<i>Cdh1</i>	Sense	5'-ATCCTCGCCCTGCTGATT-3'
	Antisense	5'-ACCACCGTTCTCCTCCGTA-3'
<i>Cftr</i>	Sense	5'-ATGTGGCCTCACTGTCCCTC-3'
	Antisense	5'-GCTGATCGAGGTCTAAGAGCA-3'
<i>Cldn2</i>	Sense	5'-TGTGAATGAAGTGAAGGAAAGC-3'
	Antisense	5'-ATCCTGCACCCAGCTGTATT-3'
<i>Cps1</i>	Sense	5'-ACT GAG AGA TGC TGA CCC TA-3'
	Antisense	5'-CCT GGA AAT TGG TGA GGA GA-3'
<i>Cyp1a2</i>	Sense	5'-CCCTGCCCTTCAGTGGTACA-3'
	Antisense	5'-AAGCTGTAGAGGTCTGGTCG-3'
<i>Cyp2e1</i>	Sense	5'-GGAACACACCTTAAGTCAGTGGACA-3'
	Antisense	5'-ATGGGTTCTTGGCTGTGTTT-3'
<i>Cyp3a11</i>	Sense	5'-TGAATATGAAACTTGCTCTCACTAAAA-3'
	Antisense	5'-CCTTGTCTGCTTAATTTCAGAGGT-3'
<i>Cyp7a1</i>	Sense	5'-TCAAGCAAACACCATTCTG-3'
	Antisense	5'-GGCTGCTTCATTGCTCA-3'
<i>Glul</i>	Sense	5'-CTCGCTCTCCTGACCTGTT-3'
	Antisense	5'-TTCAAGTGGAACTTGCTGA-3'
<i>Hnf4a</i>	Sense	5'-CAGCAATGGACAGATGTGTGA-3'
	Antisense	5'-TGGTGATGGCTGTGGAGTC-3'
<i>Gapdh</i>	Sense	5'-ACCACAGTCCATGCCATCAC-3'
	Antisense	5'-TCCACCACCCCTG TTGCTGTA-3'
<i>Lgr5</i>	Sense	5'-CTTCACTCGGTGCAGTGCT-3'
	Antisense	5'-CAGCCAGCTACCAAATAGGTG-3'
<i>Tdo2</i>	Sense	5'-TGAGTAAAGGTGAACGACGAC-3'
	Antisense	5'-AGCCGACTGAGAATCCTGTA-3'

## Supplementary Figures

Fig. S1

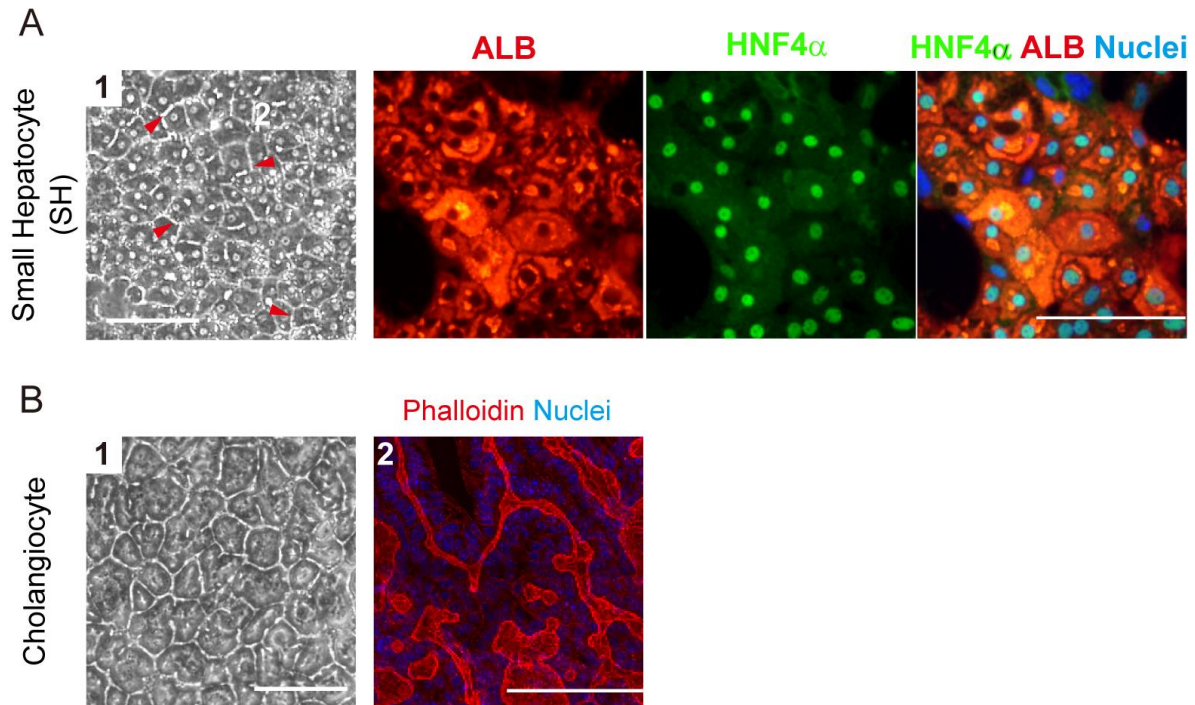


**Fig. S1. Morphogenesis of SHs and cholangiocytes in culture.**

**A. SHs differentiate to mature hepatocytes.** SHs show similar cellular morphology to MHs, including round nuclei and dense cytoplasm, in the presence of OSM and Matrigel (**panel 1**). SHs form bile canaliculi (**arrowheads**), but they are not organized into a network. SHs are positive for HNF4α and ALB (**panel 2**). SHs were cultured on gelatin-coated dishes for five days. They were further cultured in the presence of OSM for one day, and then overlaid with Matrigel. Bars represent 100  $\mu$ m.

**B. Cholangiocytes form tubular networks in sandwich culture.** Cholangiocytes proliferate on type I collagen gel and form tubular structures after overlay with collagen gel (**panel 1**). A luminal network is visualized using phalloidin (**panel 2**). Bars represent 100  $\mu$ m.

Fig. S2

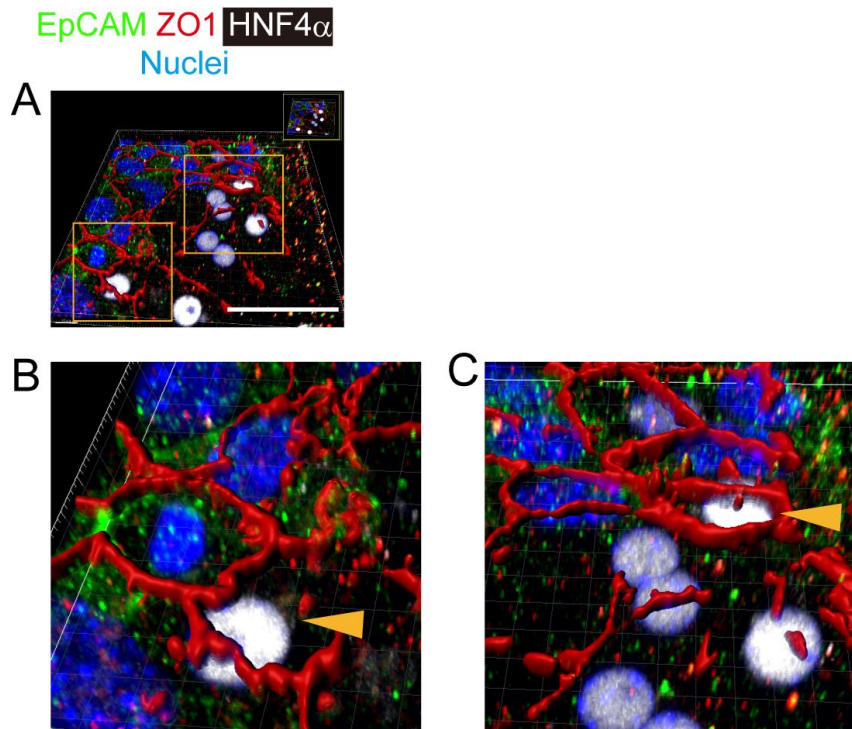
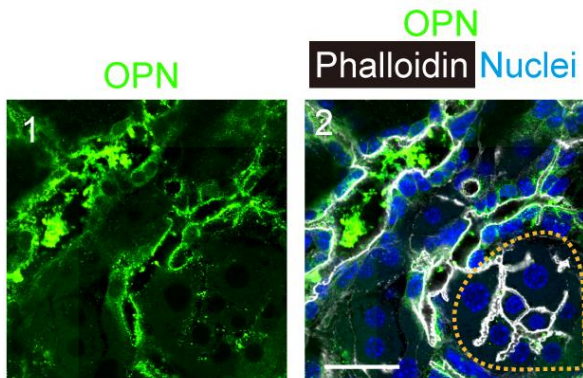


**Fig. S2. SHs and cholangiocytes quickly form intercellular junctions.**

HNF4 $\alpha$ <sup>+</sup> hepatocytes (**arrowheads in panels B&C**) form tight junctions with EpCAM<sup>+</sup> cholangiocytes. The boxes in panel A are enlarged in panels B and C. Tight junctions are visualized with ZO1 staining. A surface model was generated using Imaris software. The bar in panel A represents 50  $\mu$ m.

Fig. S3

A



B

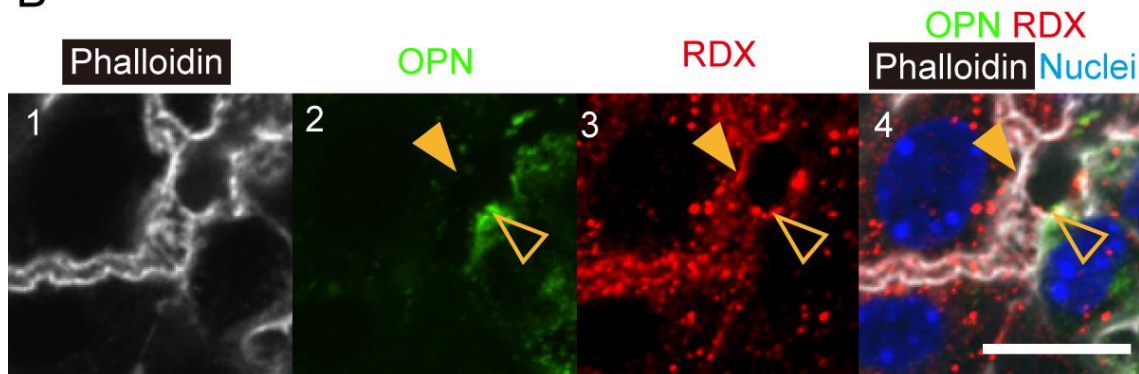
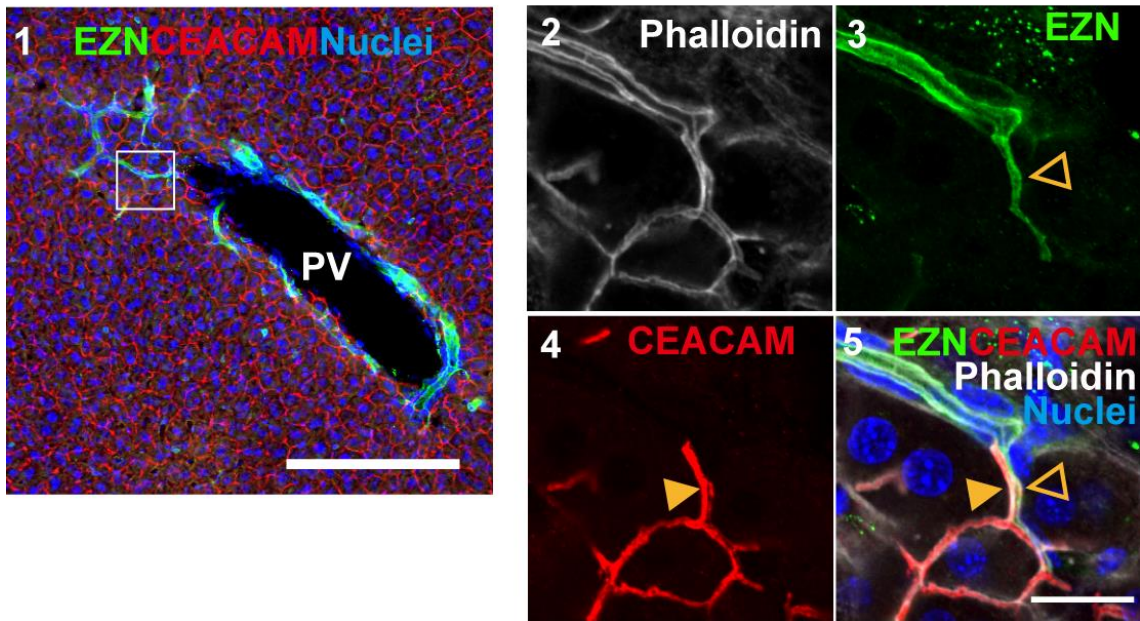


Fig. S3. Expression of OPN and RDX in HBTO.

- Cholangiocytes in HBTO express OPN.** OPN (green) is expressed in cholangiocytes but not in hepatocytes (surrounded by yellow dotted line). The bar represents 50  $\mu$ m.
- Expression of OPN and RDX in the hepatobiliary junction.** The apical membrane of an OPN<sup>+</sup> cholangiocyte and that of an RDX<sup>+</sup> hepatocyte surround the luminal structure at the hepatobiliary junction. The bar represents 20  $\mu$ m.

Fig. S4



**Fig. S4. Hepatobiliary connection *in vivo***

The canalicular membrane and the lumen of bile ducts are positive for CEACAM and EZN, respectively (panel 1). At the connection between the bile canaliculi and the bile duct, CEACAM<sup>+</sup>EZN<sup>-</sup> hepatocytes (closed arrowhead) and CEACAM<sup>-</sup>EZN<sup>+</sup> cholangiocytes (open arrowhead) surround the lumen. The box in panel 1 is enlarged in panels 2 to 5. Bars in panels 1 and 5 represent 200 and 50  $\mu$ m, respectively.

Fig. S5

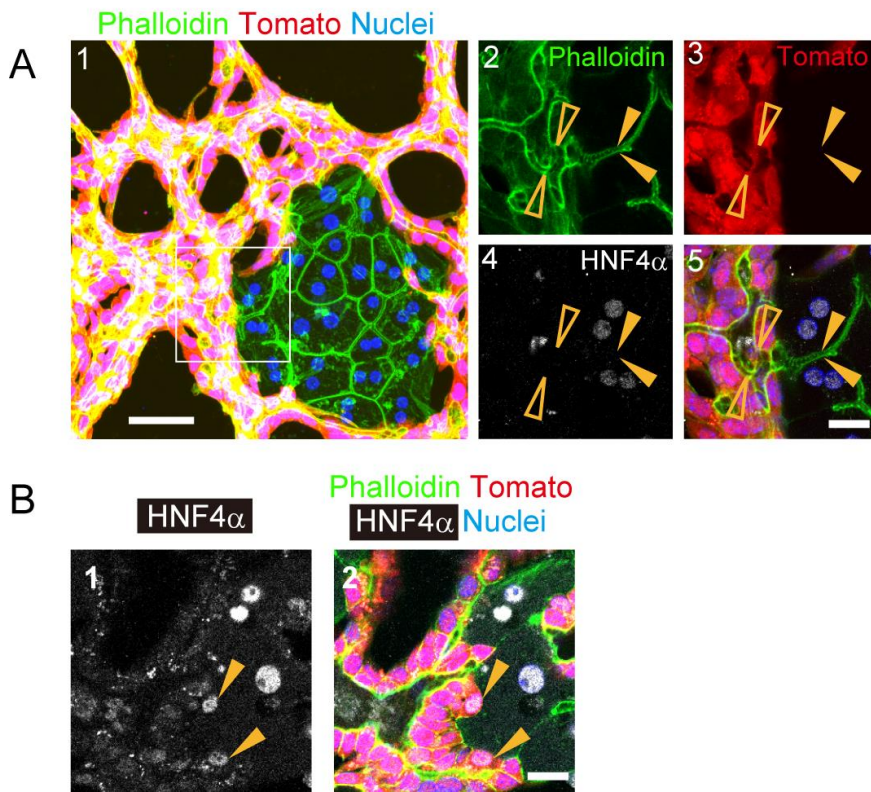


**Fig. S5. Co-culture of Tomato<sup>+</sup> cholangiocytes and wild type SHs.**

A. **Tomato<sup>+</sup> cholangiocytes maintain their lineage to form a continuous luminal network with hepatocytes.** The luminal network among Tomato<sup>-</sup>HNF4α<sup>+</sup> hepatocytes (yellow arrows) is connected to that of the Tomato<sup>+</sup> biliary structure (white arrows) at the boundary (yellow arrowheads). The luminal network is recognized by F-actin bundles visualized with AlexaFluor488-conjugated phalloidin. Bars represent 50 μm and 20 μm in panels 1 and 5, respectively.

B. **Some Tomato<sup>+</sup> cholangiocytes express HNF4α but maintain cholangiocyte morphology.** Some Tomato<sup>+</sup> cholangiocytes express HNF4α but its expression level is weak as compared with hepatocytes (arrowheads in panels 1 and 2). Those HNF4α<sup>low</sup> cells show cellular morphology identical to that of neighboring cholangiocytes. The bar represents 20 μm.

Fig. S6

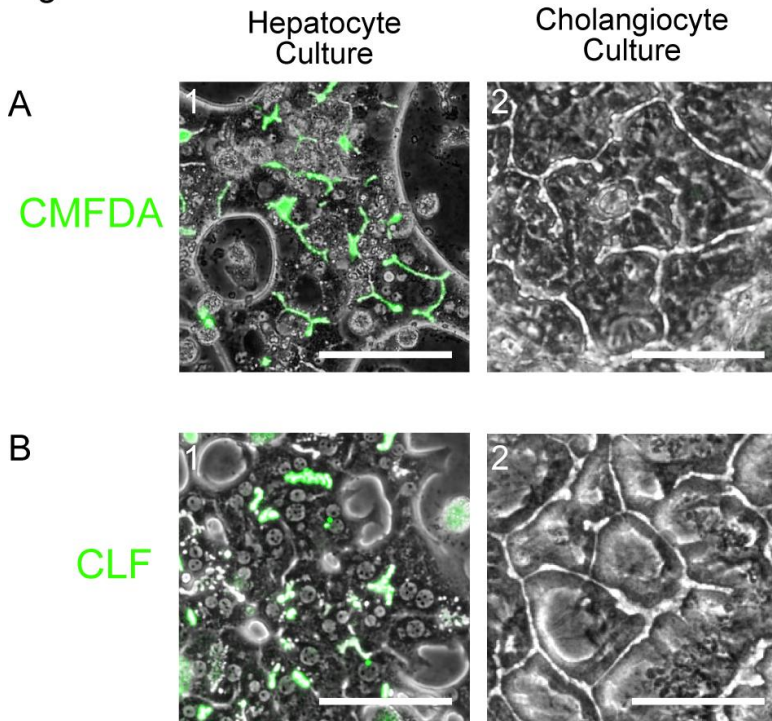


**Fig. S6. Uptake of FDA and CLF by hepatocytes and cholangiocytes.**

A. **Hepatocytes, but not cholangiocytes, take up FDA.** Hepatocytes take up chloromethylfluorescein diacetate (CMFDA), metabolize it, and secrete fluorescein into BC (**panel 1**). In contrast, cholangiocytes do not take up FDA and, therefore fluorescein does not accumulate in the luminal space (2). SHs and cholangiocytes were cultured on type I collagen gel and overlaid with collagen gel containing 20% MG. They were incubated in the medium with CMFDA for 30 min and washed five times with culture medium before images were taken using a fluorescence microscope. Bars represent 100  $\mu$ m.

B. **Hepatocytes, but not cholangiocytes, take up CLF.** Hepatocytes absorb choly-l-lysine fluorescein (CLF) and secrete it into the BC (**panel 1**). In contrast, cholangiocytes do not take up and accumulate CLF in the luminal space (**panel 2**). Hepatocytes and cholangiocytes were incubated in medium with CLF for 2 h and washed five times with culture medium before images were taken using a fluorescence microscope. Bars represent 100  $\mu$ m.

Fig. S7

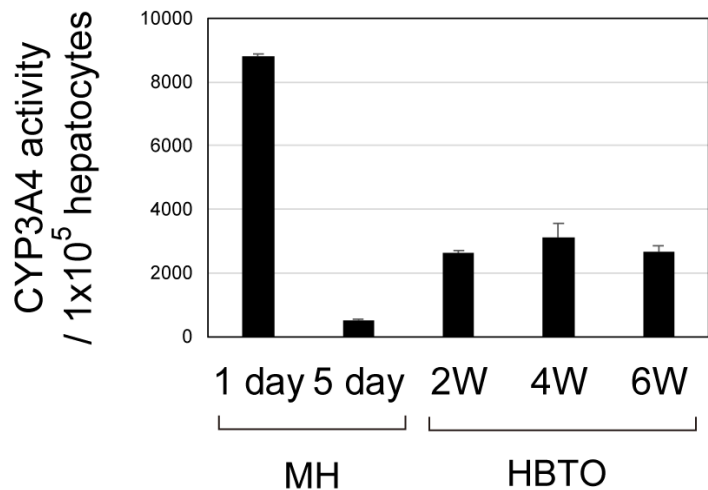
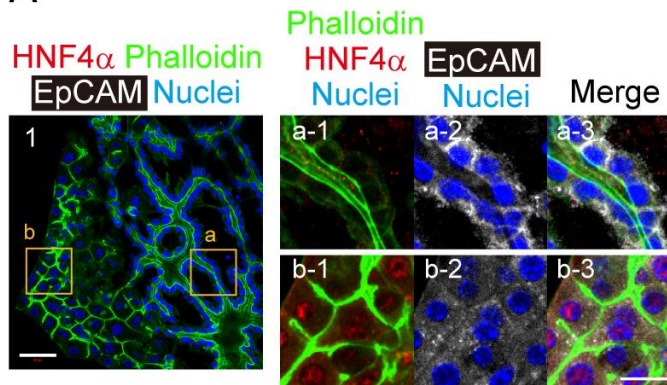


**Fig. S7. Primary MHs lose Cyp activity in culture.**

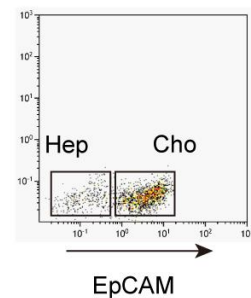
CYP3A4-like activity in MHs decline to less than one-twentieth during five days of culture. Although CYP3A4-like activity in HBTOs is about one-fourth that in MHs after one day, it is maintained for a month. Primary MHs ( $1 \times 10^5$  cells) were cultured in 24-well plates coated with type I collagen. CYP3A4-like activity was measured at one and five days after plating. HBTO were induced from SHs ( $5 \times 10^4$  cells) and cholangiocytes ( $5 \times 10^4$  cells) in 24 well plates. CYP3A4-like activity was measured in four wells of MHs and HBTO cultures, independently. The average values of CYP3A4-like activity per  $1 \times 10^5$  hepatocytes are shown in the graph. At each time point, four wells were used to measure CYP3A4 activity. Error bars represent SEM.

Fig. S8

A



B



C

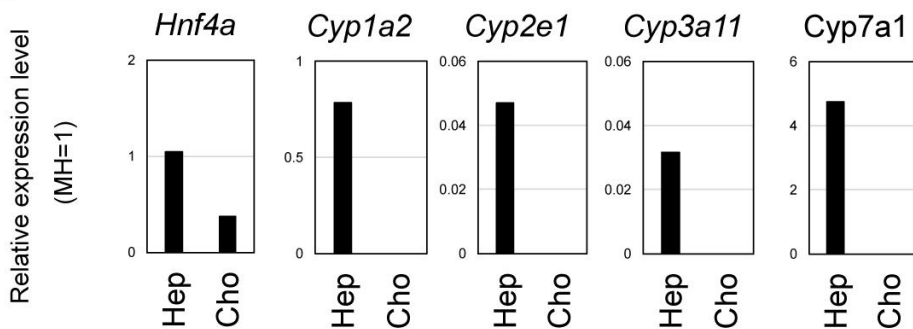
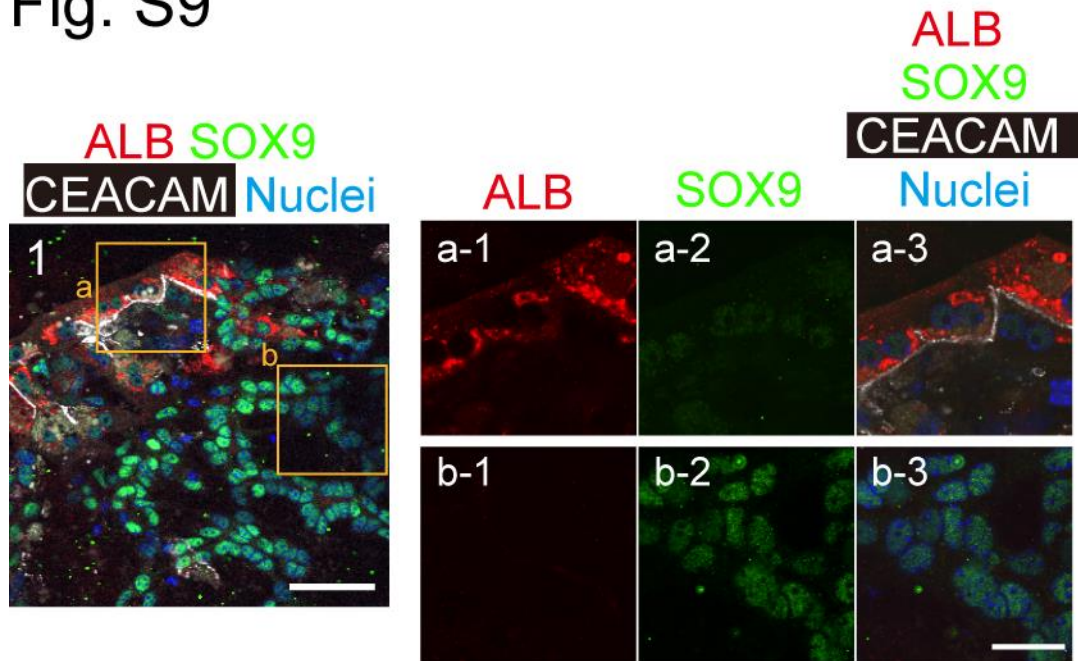


Fig. S8. Expression of hepatocyte markers in HBTOs.

- Cholangiocytes, but not hepatocytes, express EpCAM in HBTOs.** Bars in panels 1 and b-3 represent 50 and 20  $\mu$ m, respectively.
- Separation of cholangiocytes and hepatocytes derived from HBTOs.** HBTOs were digested with Liberase TM to liberate cells, and hepatocytes and cholangiocytes were isolated as EpcAM(–) and EpCAM(+) cells, respectively.
- Cyps are specifically expressed in hepatocytes in HBTO.** Expression of hepatocyte markers was examined using qPCR. The expression levels of hepatocyte markers are presented as relative values against those in MHs cultured for one day. Cell isolation was repeated twice, and representative data are shown in the graphs.

Fig. S9



**Fig. 9. ALB expression in HBTOs.**

ALB is expressed in CEACAM<sup>+</sup> hepatocytes, but not in SOX9<sup>+</sup> cholangiocytes. Boxes in panel 1 are enlarged in panels a-1 to 3 and b-1 to 3, respectively. Bars in panels 1 and b-3 represent 50 and 20  $\mu$ m, respectively.

Fig. S10

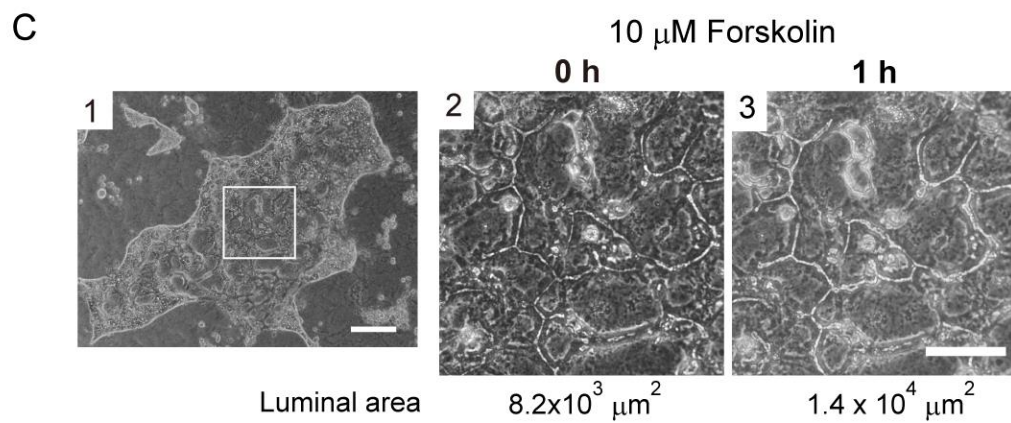
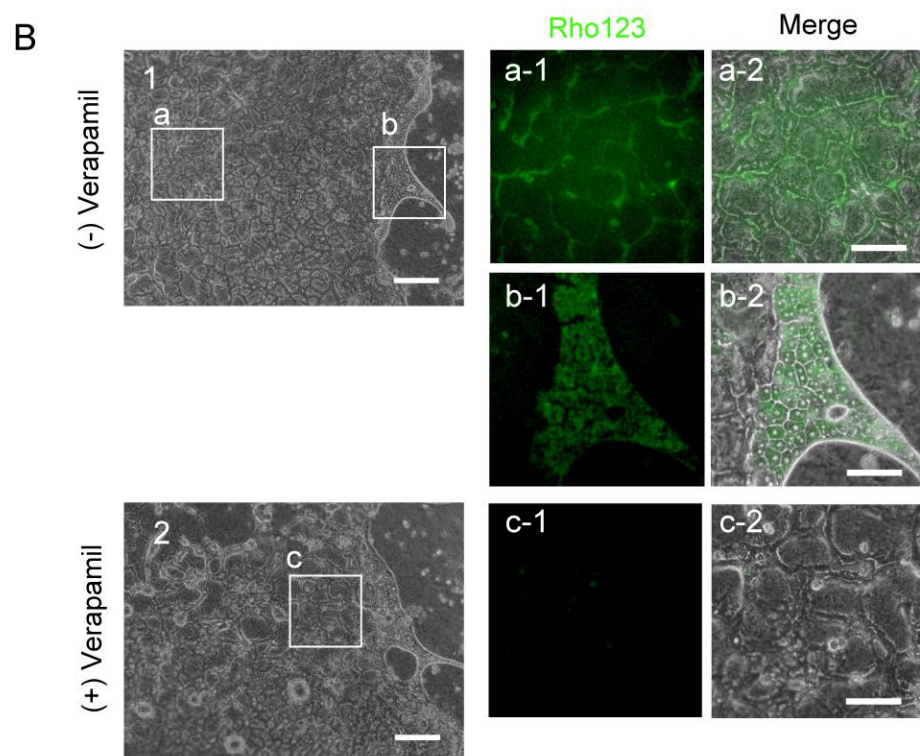
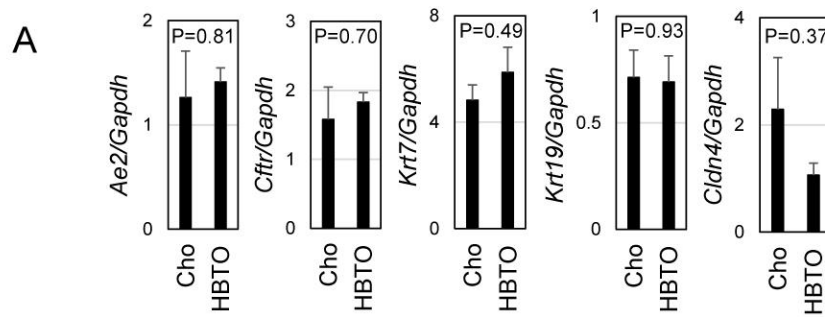


**Fig. S10. Cholangiocytes are functional in the hepatobiliary organoids.**

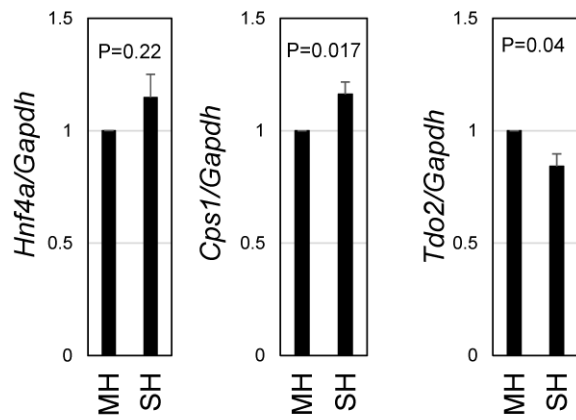
A. **Cholangiocytes in the organoids express cholangiocyte marker genes.** Expression levels of *Ae2*, *Cftr*, *Krt7*, *Krt19*, and *Cldn4* are similar between Cho and HBTO, suggesting that cholangiocytes in HBTOs maintain their cellular characteristics as differentiated cholangiocytes. Cholangiocytes were maintained in sandwich culture for four weeks, the same culture conditions as HBTOs. cDNA was prepared from four independent wells both for cholangiocytes and HBTOs, and used for qPCR analysis. Error bars represent SEM.

B. **Cholangiocytes take up Rho 123 depended on Mdr1 activity.** HBTOs were incubated in the presence of Rho123 without (**panel 1**) or with (**panel 2**) verapamil. Rho123 is absorbed by cholangiocytes and accumulated in the biliary tissue (**panels a-1 and a-2**). Rho 123 is absorbed by hepatocytes, but do not accumulate in the BC (**panels b-1 and b-2**). The accumulation of Rho123 in the biliary tissue is blocked by verapamil, a MDR1 inhibitor (**panels c-1 and c-2**). Boxes in panels 1 and 2 are enlarged in panels a-1&a-2, b-1&b-2, and c-1&c-2, respectively. Bars in panels 1 and 2 represent 200  $\mu$ m, and in panels a-2, b-2, and c-2 100  $\mu$ m.

C. **Cholangiocytes expand the luminal space in response to forskolin.** The luminal space of the biliary tissue is expanded about two-fold in the presence of forskolin. HBTOs were incubated in the presence of forskolin for one hour. The luminal space at 0 and 1 hour was quantified using ImageJ. The box in panel 1 is enlarged in panel 2 and an image of the same area at one hour is shown in panel 3. Bars in panels 1 and 3 represent 200 and 100  $\mu$ m, respectively.

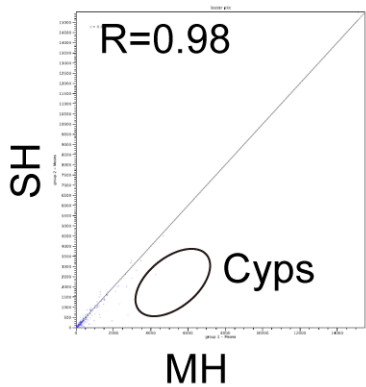
Fig. S11

A

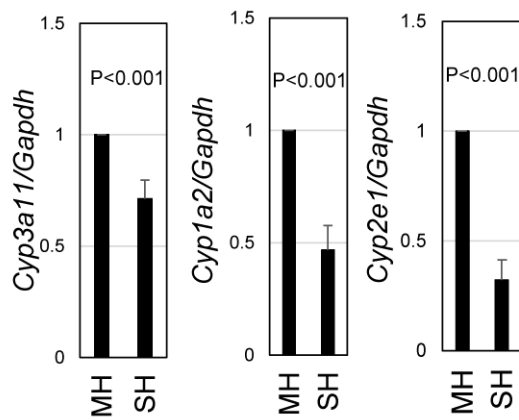


B

1

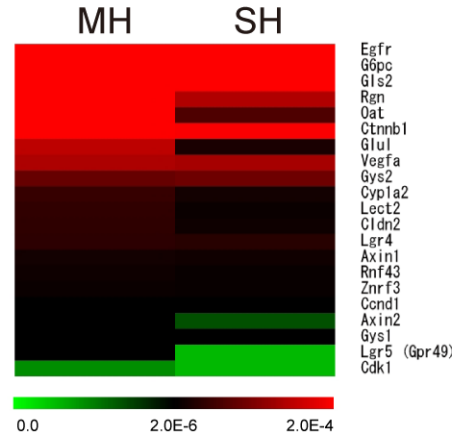


2



C

1



2

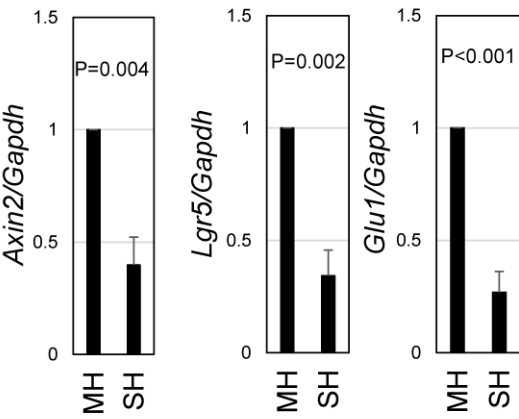


**Fig. S11. Comparison of gene expression in SHs with that of MHS.**

- A. **SHs express hepatocyte markers.** SHs express *Hnf4a*, *Cps1*, and *Tdo2* at a level comparable with that of MHS. *Cps1* is expressed slightly more highly in SHs, whereas *Tdo2* is lower in SHs than in MHS. Error bars represent SEM.
- B. **Cyps are expressed significantly less in SHs than in MHS.** RNA sequence data suggests that the expression of Cyps is lower in SHs than in MHS (panel 1). qPCR analyses further demonstrate that the expression of *Cyp3a11*, *Cyp1a2*, and *Cyp2e1* are significantly lower in SHs than in MHS. Error bars represent SEM.
- C. **WNT target genes are expressed significantly less in SHs than in MHS.** RNA sequence data suggests expression of WNT target genes is lower in SHs than in MHS (panel 1). qPCR analyses further demonstrate that the expression of *Axin2*, *Lgr5*, and *Glu1* are significantly lower in SHs than in MHS. Error bars represent SEM.

Fig. S12

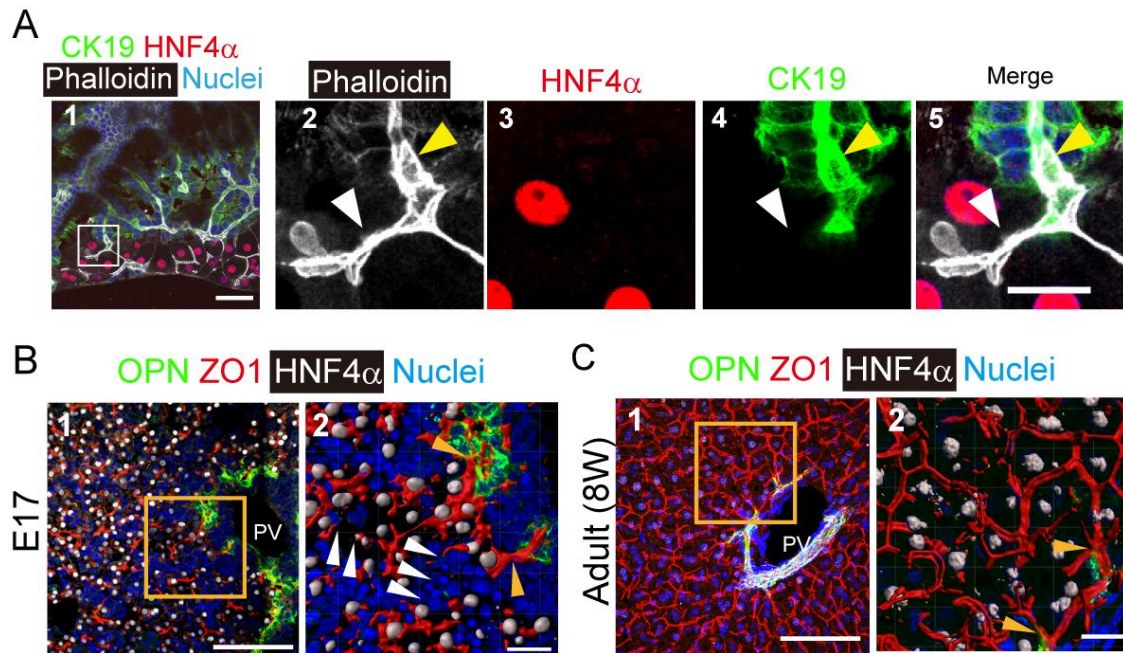


**Fig. S12. Hepatocytes and biliary epithelial cells form junctional structures at the onset of liver epithelial morphogenesis.**

**A. Hepatobiliary junctions in co-culture.** The continuous apical luminal network (green) in HNF4 $\alpha$ <sup>+</sup> hepatic cells (white arrow in panel 5) and that in CK19<sup>+</sup> biliary tissue (yellow arrow in panel 5) is already connected at 1 week after MG overlay. Bars in panels 1 and 5 represent 50 and 20  $\mu$ m, respectively.

**B. Hepatobiliary junctions in fetal liver.** The BC network is already connected to IHBDs around the portal vein at E17 (arrowhead in panels 2–4). At this stage, the BC is still discontinuous, whereas IHBDs consist of a fine homogeneous luminal network. An E17 liver was stained with anti-OPN, anti-ZO1 and anti-HNF4 $\alpha$  antibodies. The bars in panels 1 and 2 represent 100 and 20  $\mu$ m, respectively.

**C. Hepatobiliary junctions in adult liver.** The apical luminal network is continuous among

hepatic cords and IHBDs (**arrowheads in panels 2–3**). A thick tissue section of an adult liver was stained with anti-OPN (green), anti-ZO1 (red) and anti-HNF4 $\alpha$  (white) antibodies. Confocal images were collected from slices of 20  $\mu$ m thickness, and a projection image was reconstituted using Zeiss Zen software (**panel 1**). The box in panel 1 was cropped and a surface model was constructed using Imaris. The bars in panels 1 and 2 represent 100 and 20  $\mu$ m, respectively.

Fig. S13

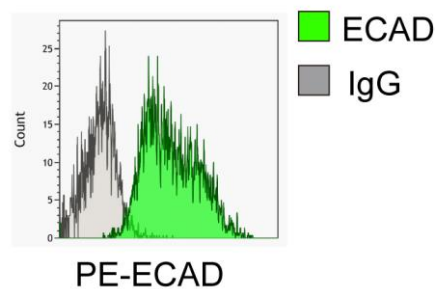


**Fig. S13. ECAD expression in cholangiocytes.**

Cholangiocytes were cultured for five days on type I collagen gel. Cholangiocytes were isolated from culture by digesting the collagen gel with Liberase TM and then examined for the expression of ECAD in FACS.